

Engineering magnetism in semiconductors

Transition metal doped III-V, II-VI, and group IV compounds offer an unprecedented opportunity to explore ferromagnetism in semiconductors. Because ferromagnetic spin-spin interactions are mediated by holes in the valence band, changing the Fermi level using co-doping, electric fields, or light can directly manipulate the magnetic ordering. Moreover, engineering the Fermi level position by co-doping makes it possible to modify solubility and self-compensation limits, affecting magnetic characteristics in a number of surprising ways. The Fermi energy can even control the aggregation of magnetic ions, providing a new route to self-organization of magnetic nanostructures in a semiconductor host.

Tomasz Dietl¹ and Hideo Ohno²

¹Laboratory for Cryogenic and Spintronic Research, Institute of Physics, Polish Academy of Sciences and ERATO Semiconductor Spintronics Project, Japan Science and Technology Agency, 02-668 Warszawa, Poland
Institute of Theoretical Physics, Warsaw University, 00-681 Warszawa, Poland
E-mail: dietl@ifpan.edu.pl

²Laboratory for Nanoelectronics and Spintronics, Research Institute of Electrical Communication, Tohoku University and ERATO Semiconductor Spintronics Project, Japan Science and Technology Agency, Sendai 980-8577, Japan
E-mail: ohno@riec.tohoku.ac.jp

Over the past two decades, spintronic research has spread to all branches of condensed matter physics and materials science. Because of the asymmetry in the monopole nature of electric charges versus the dipole nature of magnetic charges, magnetic dipoles are not easily shielded. Yet random magnetic fields are weaker than random electric fields, so the electron spin may in the end be a better information carrier than the electron charge in classical technologies let alone quantum information processing.

Metal magnetic multilayers, in which spin-dependent electron scattering and tunneling are at work, are now well developed and used in the read heads of hard disks and in magnetic random access

memories (MRAMs) that are reaching the production stage.

Ferromagnetic semiconductors are on the research and development horizon and combine the properties of ferromagnetic and semiconducting systems at the material level. So far only displays of (Zn,Mn)S and Faraday optical insulators of (Cd,Mn)Te and related compounds have been developed as spintronic devices containing magnetically doped semiconductors as the working element. As such, semiconductor spintronics¹⁻⁴ is at a nascent but fascinating stage, where many important material developments lie ahead.

Early studies on ferromagnetic semiconductors such as Cr spinels and rock salt Eu- and Mn-based chalcogenides led to the observation of

a number of phenomena associated with the interplay between ferromagnetism and semiconducting properties. A strong spin-dependent (exchange) coupling between the ordinary semiconductor band carriers and spins localized on the magnetic atoms accounts for the unique properties of these materials⁵. This coupling gives rise to strong indirect exchange interactions between the localized moments, as well as giant spin-splitting of the electronic states proportional to the magnetization of the spins.

The discovery of carrier-controlled ferromagnetism in Mn-based zinc-blende III-V compounds^{6,7}, such as (In,Mn)As and (Ga,Mn)As, followed by the prediction⁸ and observation^{9,10} of ferromagnetism in *p*-type II-VI materials, such as (Cd,Mn)Te and (Zn,Mn)Te:N, has allowed one to explore the physics and possible applications of previously unavailable combinations of quantum structures and ferromagnetism in semiconductors. Owing to novel functionalities¹¹ and theoretical expectations¹², efforts worldwide are now being directed at developing diluted magnetic semiconductors (DMS) that sustain ferromagnetism at high temperatures¹³⁻¹⁷ and at describing their properties theoretically¹⁸.

Ferromagnetic response, often persisting above room temperature, has been detected in a large number of semiconductor and oxide thin layers containing a minute amount of magnetic ions¹³⁻¹⁷ or even when nominally undoped by magnetic elements¹⁹. A highly sensitive, superconducting quantum interference device (SQUID) magnetometer is necessary to detect the correspondingly small signals, which are often smaller than those coming from a typical remanent field, sample holder, substrate, or residual magnetic nanoparticles originating from nominally nonmagnetic source materials or processing procedures²⁰. In rather rare cases, the ferromagnetic signal of DMS layers can be unequivocally assigned to precipitates of a known ferromagnetic or ferrimagnetic material. In a few other cases, the magnitude of the ferromagnetic signal is greater than that evaluated from the nominal concentration of magnetic ions. More often, however, the ferromagnetic response of the layer coexists with paramagnetic characteristics, indicating that only a fraction of the magnetic spins remain correlated at high temperatures.

In this review, we describe properties and functionalities of DMS in which long-range ferromagnetic interactions are mediated by valence-band holes. In such systems, a shift of the Fermi level by co-doping, electric field, or light alters the ordering temperature and the magnetization direction. We discuss how Fermi-level engineering in wide-bandgap semiconductors and oxides can modify self-compensation and spinodal decomposition, which in turn can serve to control the positions and aggregation of magnetic ions. The resulting self-organized growth of magnetic nanocrystals inside a nonmagnetic matrix explains, according to recent work, the outstanding properties of a broad class of high-temperature ferromagnetic semiconductors and oxides. At the same time, enhanced magneto-optical and magnetotransport properties of these composite

materials systems opens the door for their applications in photonic and storage devices.

Carrier-controlled ferromagnetic DMS

Owing to the short-range character of the direct exchange interaction between tightly localized magnetic orbitals, the coupling between *d* spins proceeds indirectly via *sp* bands in tetrahedrally coordinated DMS²¹. Such a coupling is usually antiferromagnetic, if the *sp* bands are either entirely occupied or totally empty (superexchange), but can acquire a ferromagnetic character in the presence of free carriers.

It is well established that Mn is divalent in II-VI compounds and assumes the high-spin *d*⁵ configuration characterized by $S = 5/2$. Here, Mn ions neither introduce nor bind carriers, but give rise to the presence of localized spins. For low carrier densities, the magnetic susceptibility of II-VI DMS shows a Curie-Weiss dependence characterized by an antiferromagnetic Curie-Weiss temperature T_{AF} and a reduced Mn concentration, as neighboring Mn-Mn pairs are antiferromagnetically blocked owing to the short-range superexchange interactions. However, this antiferromagnetic coupling can be overcompensated by ferromagnetic interactions mediated by band holes^{9,22}. In III-V compounds, Mn atoms that substitute trivalent metals supply both localized spins and holes, so that extrinsic co-doping is not necessary to generate the carrier-mediated spin-spin interaction²³.

In the 1950s, Zener noted the role of band carriers in promoting ferromagnetic ordering between localized spins in magnetic metals. This ordering can be viewed as being driven by the lowering of the carriers' energy associated with their redistribution between spin subbands, split by the exchange coupling to the localized spins (Fig. 1). A more detailed quantum treatment indicates, however, that the sign of the interaction between localized spins oscillates with their distance according to the Ruderman-Kittel-Kasuya-Yosida (RKKY) model. Because of the large density of states and spin-dependent hybridization between anion *p* and magnetic *d* states, the carrier-mediated spin-spin interaction is particularly strong in the presence of holes in tetrahedrally coordinated DMS⁸. Interestingly, this carrier-mediated Zener/RKKY ferromagnetism is enhanced by exchange interactions within the carrier liquid⁸. These interactions account for ferromagnetism in metals (the Stoner mechanism) and contribute to the magnitude of the Curie temperature T_C in ferromagnetic semiconductors.

Guided by the growing number of experimental results, including informative magnetic resonance^{24,25} and photoemission²⁶⁻²⁹ studies, a theoretical model of hole-controlled ferromagnetism in III-V, II-VI, and group IV semiconductors containing Mn has been proposed^{12,30,31}. The theory is built on Zener's *p-d* model of carrier-mediated ferromagnetism and either Kohn-Luttinger's *kp*^{12,30,31} or multiorbital tight-binding³²⁻³⁴ descriptions of the valence band in tetrahedrally coordinated semiconductors. It has qualitatively, and often

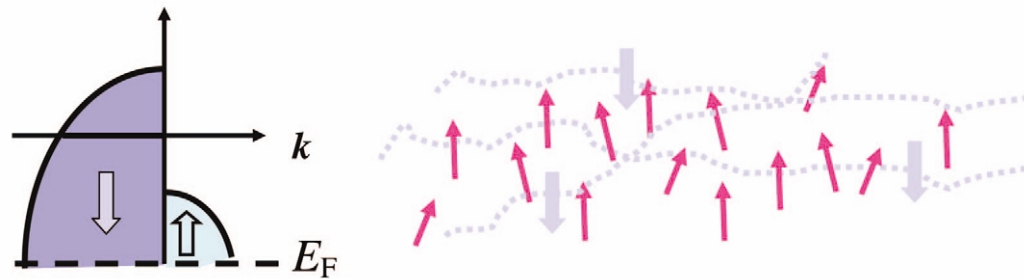


Fig. 1 Representation of carrier-mediated ferromagnetism in p-type DMS, a model proposed originally by Zener for metals. Owing to the p-d exchange interaction, ferromagnetic ordering of localized spins (red arrows) leads to spin splitting of the valence band. The redistribution of the carriers between spin subbands lowers the energy of the holes, which at sufficiently low temperatures overcompensates an increase of the free energy associated with a decrease in Mn entropy.

quantitatively, described thermodynamic, micromagnetic, transport, and optical properties of DMS with delocalized holes^{12,18,30,35-37}, challenging competing theories. It is often argued that, owing to these studies, (Ga,Mn)As has become one of the best-understood ferromagnets. Accordingly, this material now serves as a testing ground for various *ab initio* computation approaches to strongly correlated and disordered systems.

It should be emphasized that this description of ferromagnetic DMS is strictly valid only in the weak coupling limit, where virtual-crystal and molecular-field approximations can be made for alloy and spin disorder¹². On going from the antimonides to nitrides, or from tellurides to oxides, the p-d hybridization increases. The issue of how various corrections to the mean-field p-d Zener model^{5,12,18} affect theoretical values of T_C was recently examined in some detail for (Ga,Mn)As³⁷, with the conclusion that the overall picture remains quantitatively valid. Fig. 2 shows one of the recent theoretical models

for T_C compared with experimental findings for (Ga,Mn)As³⁷. These results confirm, in particular, that T_C values above 300 K could be achieved in Ga_{0.9}Mn_{0.1}As, if such a large substitutional Mn concentration is accompanied by a corresponding increase in the hole density¹².

As depicted in Fig. 3, a good description of the experimentally observed ordering temperature has also been found in the case of p-type (II,Mn)VI DMS^{9,10,38}, though in the studied tellurides, T_C is determined by a subtle interplay between short-range antiferromagnetic superexchange and long-range Zener/RKKY interactions^{9,10,22,38,39}. Furthermore, interesting effects of hole localization, leading to characteristics that are similar to colossal magnetoresistance oxides, show up at low carrier densities^{10,38-40}. At the same time, it has been demonstrated that ferromagnetism in n-type uniform DMS can be observed only at very low temperatures^{41,42}.

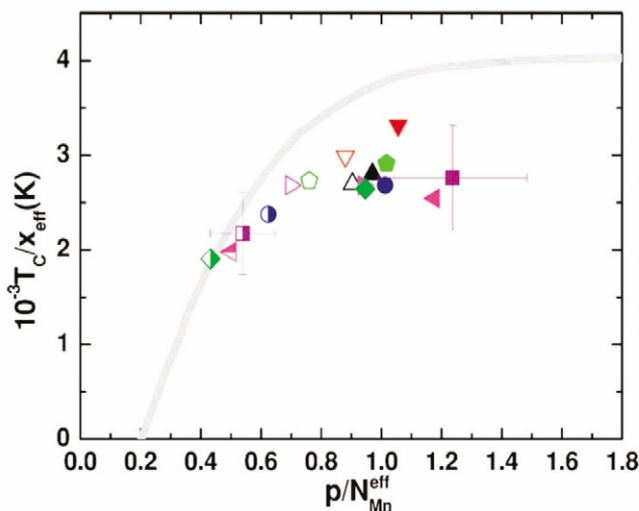


Fig. 2 Experimental Curie temperatures T_C versus hole density p for various effective concentrations of Mn moments, $N_{Mn} = 4x_{eff}/a_0^3$, where x_{eff} is the Mn content in substitutional positions and a_0 is the lattice constant. The theoretical computed T_C using the tight binding and coherent potential approximations is shown by the gray line. (Adapted and reprinted with permission from³⁷. © 2005 American Physical Society.)

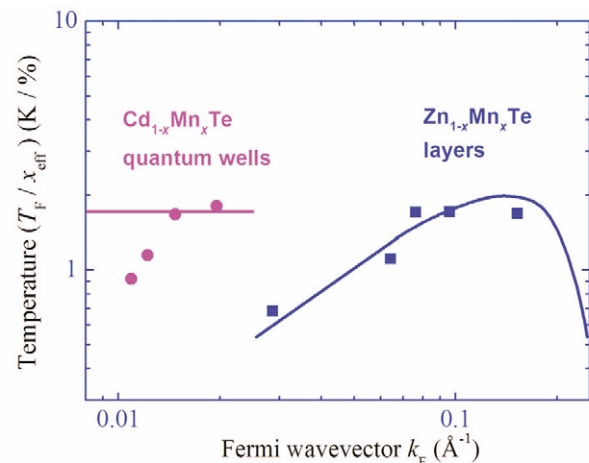


Fig. 3 Experimental (symbols) and calculated (curves) normalized ferromagnetic temperatures, $T_F = T_C - T_{AF}$, where x_{eff} is the Mn content excluding the antiferromagnetically coupled nearest-neighbor Mn pairs, versus the wave vector of holes at the Fermi level for modulation-doped p-Cd_{1-x}Mn_xTe quantum wells^{9,38} and Zn_{1-x}Mn_xTe:N epilayers¹⁰. Theory^{8,10} neglects the effects of hole localization at low densities.

Spin injection and magnetization manipulation

A large effort has been devoted to developing devices capable of injecting spins into nonmagnetic semiconductors. Owing to a high degree of spin polarization and resistance matching, ferromagnetic semiconductors constitute a natural material of choice here. Typically, a p - i - n light-emitting diode structure is employed as a spin-polarization detector in which the p -type spin-injecting electrode is a ferromagnetic semiconductor. Importantly, injection of spin-polarized electrons using Zener or Esaki tunneling from a p -type (Ga,Mn)As electrode into n -type GaAs has also been realized. A recent example of such a device is shown in Fig. 4.

Since magnetic properties are controlled by band holes, an appealing possibility is to influence the magnetic ordering isothermally using light or an electric field, which – owing to the relatively small carrier concentrations in semiconductor structures – has a much greater effect than in the case of metals.

Such tuning capabilities in the materials systems in question have been demonstrated using (In,Mn)As/(Al,Ga)Sb^{11,44} and modulation-doped p -(Cd,Mn)Te/(Cd,Mg,Zn)Te^{9,38} heterostructures (Figs. 5 and 6). These findings can be quantitatively interpreted by considering the effect of the electric field or illumination on the hole density under stationary conditions and, therefore, on T_C in the relevant magnetic layers. Interestingly, according to experimental findings and theoretical modeling, photocarriers generated in II-VI systems by above-barrier illumination destroy ferromagnetic order in a magnetic quantum well within an undoped (intrinsic) region of a p - i - p structure^{9,38}, but they enhance the magnitude of spontaneous magnetization in p - i - n diodes³⁸ (Fig. 6). Furthermore, it has been demonstrated that the electric current can reverse magnetization in trilayer structures of (Ga,Mn)As^{45,46} and displace a magnetic domain wall in this system^{47,48} (Fig. 7). It is worth mentioning that the small value of spontaneous magnetization in ferromagnetic semiconductors dramatically reduces the current density required for switching compared with metallic structures.

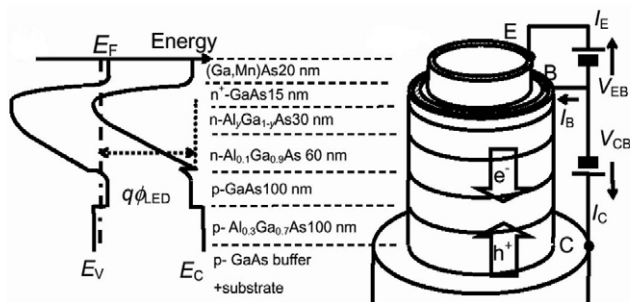


Fig. 4 (a) Schematic band diagram and (b) three-terminal device containing an Esaki diode for the injection of spin-polarized electrons via Zener tunneling from (Ga,Mn)As. The degree of spin polarization is detected by the light-emitting diode⁴³.

For the valence band states, where the periodic part of the Bloch functions contain spin components mixed up by the spin-orbit interaction (even for an isotropic Heisenberg-like interaction between the carrier and localized Mn spins), the exchange splitting of the valence band does not depend only on the product of the p - d exchange integral and the Mn magnetization, but also on the magnitude and direction of the hole wave vector, confinement, and strain. In particular, both experimental and theoretical results

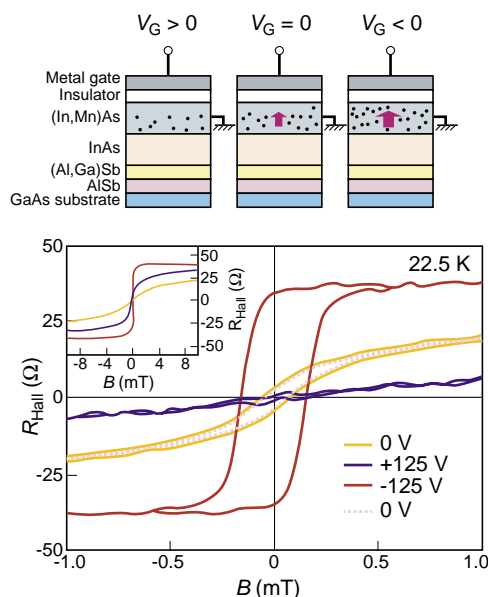


Fig. 5 Magnetization hysteresis loops determined by measurements of the anomalous Hall effect at a constant temperature of 22.5 K for various gate voltages in a field-effect transistor with an (In,Mn)As channel¹¹. The data in a wider field range are shown in the inset.

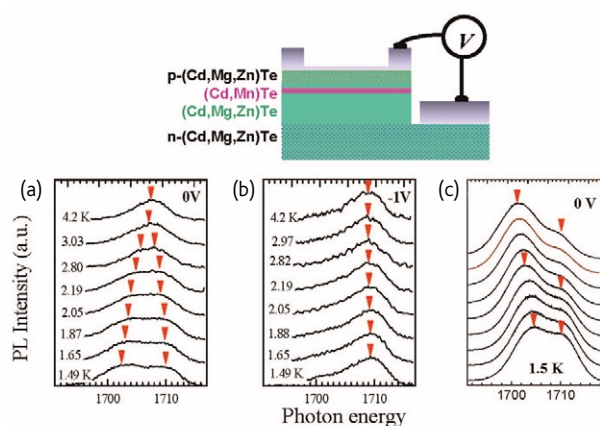


Fig. 6 Effect of (a) temperature, (b) bias voltage, and (c) illumination on the photoluminescence of a structure consisting of a modulation-doped p -(Cd,Mn)Te quantum well and n -type barrier. Zero-field line splitting (a, marked by arrows) shows the appearance of ferromagnetic ordering that does not show up if the quantum well is depleted of holes by reverse bias of the p - i - n diode (b). Low-temperature splitting is enhanced by additional illumination using white light (c), which increases hole concentration in the quantum well³⁸.

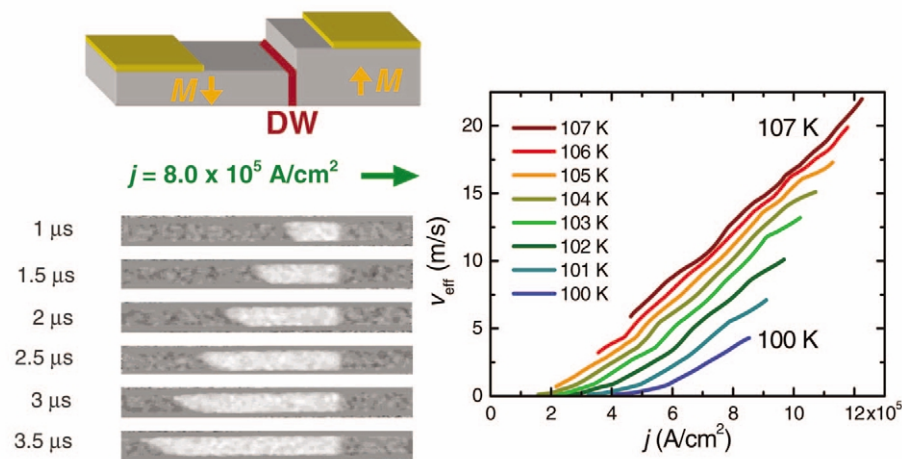


Fig. 7 A domain wall pinned by the step in a (Ga,Mn)As film with perpendicular magnetic anisotropy (top left) can be shifted by microsecond pulses of electric current, as revealed by Kerr reflectivity images (bottom left). (Right) Domain-wall velocity versus current at various temperatures⁴⁸.

demonstrate that the orientation of the easy axis with respect to the film plane depends on whether the epitaxial strain is compressive or tensile³⁰. Hence, magnetic anisotropy and, thus, easy axis direction and domain structure^{30,31,49} can be manipulated by an appropriate layout of the layer sequence, as epitaxial growth of DMS films in question is usually pseudomorphic (i.e. the subsequent layers assume the (lateral) lattice constant of the substrate by elastic deformation and no misfit dislocations are formed). Furthermore, magnetic anisotropy at a given strain is predicted to vary with the degree of the occupation of particular hole subbands. This, in turn, is determined by the ratio of the valence band exchange splitting to the Fermi energy, and thus, by the magnitude of spontaneous magnetization, which depends on temperature. Such temperature-induced switching of the easy axis direction has been detected in samples with appropriately low hole densities^{35,50}. The sensitivity of the easy axis direction to the carrier concentration constitutes a novel method for controlling the local magnetization direction by a system of electrostatic gates.

Toward room-temperature ferromagnetic DMS

In view of the potential for novel devices and system architectures, it is desirable to develop functional semiconductor systems with T_C comfortably exceeding room temperature, and in which semiconductor and magnetic properties can be controlled on an equal footing. Two strategies have been proposed to accomplish this objective¹².

The first was to increase Mn and hole concentrations in the established carrier-controlled ferromagnets, such as (Ga,Mn)As. According to the growth diagram depicted in Fig. 8, the temperature window for epitaxy of $\text{Ga}_{1-x}\text{Mn}_x\text{As}$ shrinks with x , so that it appears difficult to avoid the presence of roughening or MnAs precipitates when attempting to go beyond $x = 0.08$. Fig. 9 presents state-of-the-

art results⁵² for (Ga,Mn)As with a peak value of $T_C = 173$ K at $x = 0.08$, which is slightly above earlier findings⁵³⁻⁵⁵.

The second strategy was to develop new DMS characterized by strong p - d hybridization, large density of states, and weak spin-orbit interactions, in which T_C can be large even at moderate values of x and p . It was, however, obvious that such a program would face a number of obstacles¹², such as tight binding of holes by magnetic ions in the limit of strong p - d coupling, as well as self-compensation and solubility limits, which we discuss in the next two sections.

Controlling self-compensation

An important material issue in ferromagnetic DMS is the existence of an upper limit for the achievable carrier density under thermal equilibrium conditions. Such a limit can be caused by a finite solubility of a given dopant in a given host. In most cases, however, the effect of self-compensation is involved, which consists of the appearance of compensating point defects once the Fermi level reaches a sufficiently high position in the conduction band (donor doping) or low energy in the valence band (acceptor doping).

According to particle-induced X-ray emission (PIXE)⁵⁶, an increase in Mn concentration in (Ga,Mn)As not only results in the formation of MnAs precipitates⁵⁷ but also in Mn occupation of interstitial positions Mn_i . Since the latter has two unbound $4s$ electrons, it acts as a double donor in GaAs⁵⁸. Its formation is triggered by a lowering of the system energy caused by removal of the holes from the Fermi level. Moreover, a symmetry analysis demonstrates that the hybridization between the hole p bands and Mn_i d states is weak and the exchange interaction between Mn_i and Mn_{Ga} is antiferromagnetic⁵⁹.

The presence of interstitials appears to explain, therefore, the reentrance of the insulator phase for large Mn concentrations²³, as well as a substantial increase in magnitude of both T_C and spontaneous magnetization on annealing⁵²⁻⁵⁶ at temperatures much lower than

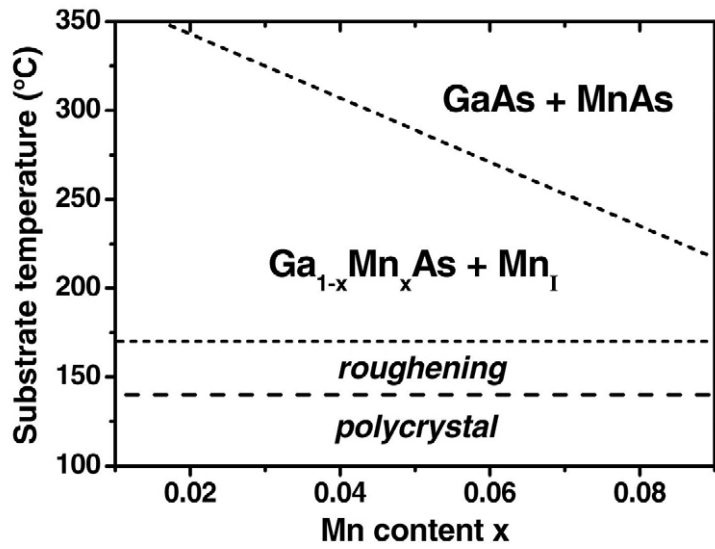


Fig. 8 Schematic of the temperature window for molecular beam epitaxy growth of (Ga,Mn)As epilayers. With the increase of the Mn content x the window shrinks and the concentration of Mn interstitials Mn_I increases⁵¹.

those affecting other known donor defects in GaAs, such as As antisites As_{Ga} . It has been demonstrated that the unwanted Mn diffuses toward the surface under annealing, where it is oxidized⁶⁰.

Compensation of holes by co-doping with, for example, Sn or H destroys ferromagnetism in (Ga,Mn)As^{61,62}, in agreement with the notion that valence band holes are necessary to mediate long-range ferromagnetic coupling between the diluted Mn spins. At this point, a natural question arises as to whether co-doping of (Ga,Mn)As by nonmagnetic acceptors, say Be, could enlarge T_C .

It has been found, in agreement with the self-compensation scenario, that the presence of additional holes during the growth of (Ga,Mn)As layer increases the Mn_I concentration, so that T_C is actually reduced^{63,64}. However, T_C is increased if additional holes are transferred to the (Ga,Mn)As layer after its epitaxy has been completed. Such engineering of ferromagnetism in $Ga_{1-y}Al_yAs$ / (Ga,Mn)As/ $Ga_{1-y}Al_yAs$ quantum structures is shown in Fig. 10. Modulation doping of Be in the back barrier diminishes T_C , as the Fermi level assumes a high position during the subsequent growth of the (Ga,Mn)As layer, resulting in Mn_I formation. In contrast, when Be is introduced in the front barrier, i.e. after the growth of (Ga,Mn)As, the concentration of Mn_I is small and T_C is increased.

Controlling the solubility limit

Another well-known difficulty in the development of functional DMS is the limited solubility of transition metals in semiconductors, which rarely exceeds a few percent, except for Mn in II-VI compounds. Various scenarios are possible if the concentration of the magnetic constituent is greater than the solubility limit under given growth conditions. One is precipitation of the magnetic element or a magnetic

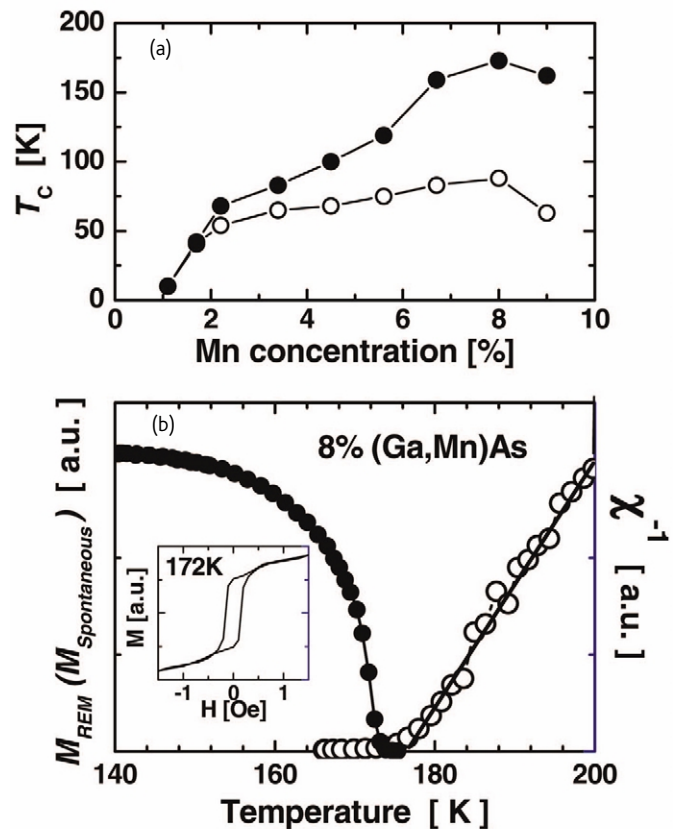


Fig. 9 (a) T_C for as-grown $Ga_{1-x}Mn_xAs$ films (empty symbols) and annealed at low temperatures (full symbols). (b) Remanent magnetization (full symbols), inverse magnetic susceptibility (empty symbols), and hysteresis loop (inset) obtained from SQUID measurements of a $Ga_{0.92}Mn_{0.08}As$ film after annealing. The data point to $T_C = 173$ K, close to the Curie-Weiss temperature⁵².

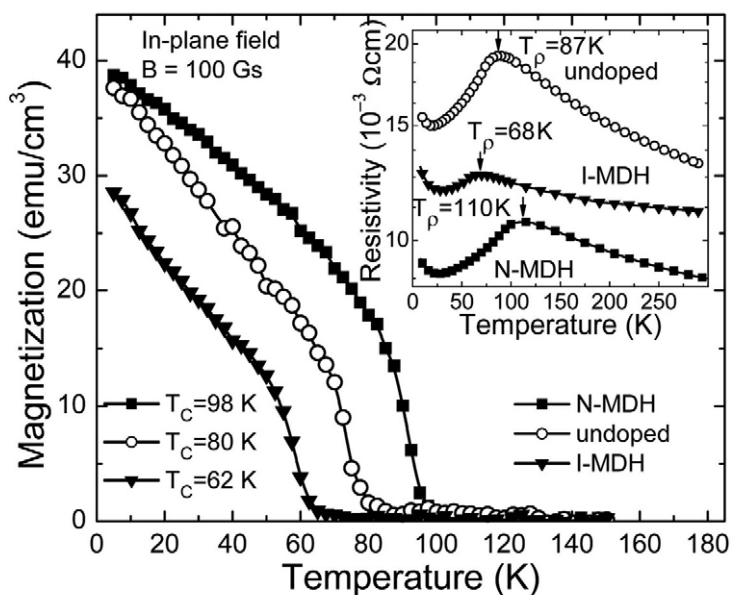


Fig. 10 Temperature dependencies of remanent magnetization and resistivity (inset) for three $\text{Ga}_{0.76}\text{Al}_{0.24}\text{As}/\text{Ga}_{1-x}\text{Mn,As}/\text{Ga}_{0.76}\text{Al}_{0.24}\text{As}$ quantum well (QW) structures. The width of the QW is 5.6 nm, $x = 0.06$. Be acceptors were introduced either into the first barrier (grown before the ferromagnetic QW), into the second barrier (grown after the ferromagnetic QW), or the sample was undoped as marked. (Adapted and reprinted with permission from⁶³. © 2003 American Institute of Physics.)

compound involving semiconductor components. Another is spinodal decomposition into regions with low and high concentrations of a particular constituent. In cases where the concentration of one of the constituents is small, this could lead to the formation of coherent nanocrystals within a majority phase. For instance, such spinodal decomposition is known to occur in epitaxially grown (Ga,In)As where In-rich quantum-dot-like regions are embedded within an In-poor matrix. *Ab initio* calculations^{65,66} have revealed a particularly strong tendency of DMS to form nonrandom alloys.

Spinodal decomposition does not usually involve the precipitation of another crystallographic phase and is, therefore, not easy to detect experimentally. Nevertheless, it has been observed in electron transmission microscopy in (Ga,Mn)As, where coherent zinc-blende Mn-rich (Mn,Ga)As nanocrystals^{67,68} lead to an apparent T_C of 360 K (Fig. 11). Furthermore, a synchrotron radiation microprobe examination⁶⁹ reveals the presence of Mn-rich nanocrystals in the host hexagonal structure of (Ga,Mn)N. A similar effect has been observed in (Ge,Mn)⁷⁰. It has, therefore, been proposed that nanoclusters with a large concentration of the magnetic constituent account for the high apparent T_C of a large class of DMS and related oxides¹⁵ in which the average concentration of magnetic ions is far below the percolation limit for nearest-neighbor coupling and, at the same time, the free-carrier density is too low to mediate an efficient long-range exchange interaction. It is worth recalling that uncompensated spins at the surface of antiferromagnetic nanocrystals can also produce a sizable spontaneous magnetization at high temperatures⁷¹. Remarkably, the presence of magnetic nanocrystals leads to an enhanced magneto-

optical⁶⁸ and magnetotransport^{72,73} response. This opens the door for various applications of such hybrid systems, including magneto-optical spatial light modulators for volumetric recording, providing that methods for controlling the nanocrystal growth can be found.

The energy levels derived from the open d shells of transition metals usually reside in the band gap of the host semiconductor. This property is already exploited in the fabrication of semi-insulating

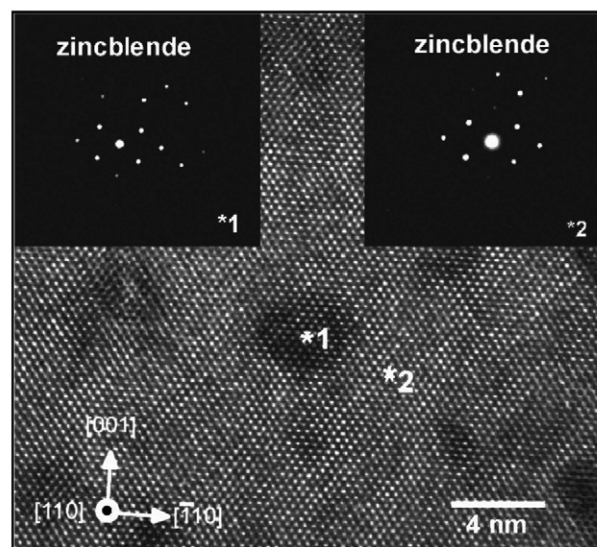


Fig. 11 Transmission electron micrograph and two diffraction patterns of an annealed (Ga,Mn)As sample. Diffraction patterns are taken from an MnAs cluster (*1) and the GaAs matrix (*2). (Adapted and reprinted with permission from⁶⁸. © 2005 American Institute of Physics.)

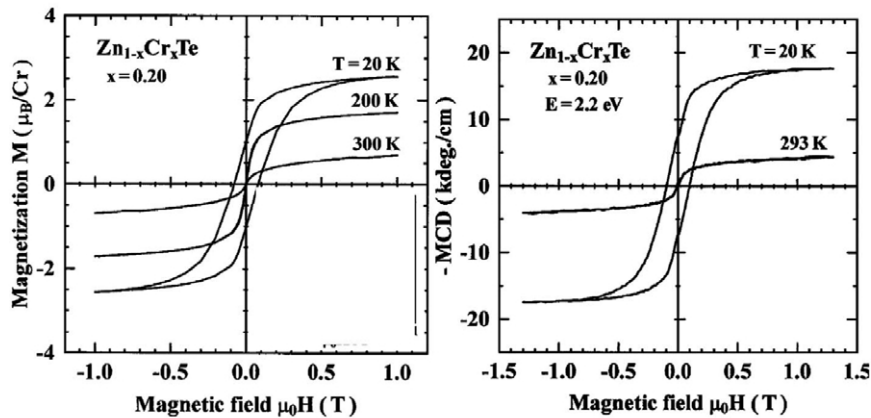


Fig. 12 (a) Magnetic field dependence of magnetization, and (b) intensity of magnetic circular dichroism (MCD) at photon energy 2.2 eV at various temperatures T for $\text{Zn}_{0.8}\text{Cr}_{0.2}\text{Te}$ film. (Adapted and reprinted with permission from⁷⁶. © 2003 American Physical Society.)

materials, where the midgap levels of magnetic impurities trap carriers originating from residual impurities or defects. It has been suggested⁷⁴ that such trapping alters the charge state of the magnetic ions and hence affects their mutual Coulomb interactions. These interactions are not screened out in materials with small carrier concentrations and, therefore, the intersite Coulomb repulsion can overcompensate the lowering of the free energy arising from the nearest-neighbor bonding. This impedes spinodal decomposition and stabilizes the growth of a uniform alloy, even if the concentration of the constituents lies within the solubility gap for the isoelectronic compound.

Accordingly, intentional co-doping of DMS with shallow acceptors or donors could provide a means for precluding or promoting the ion aggregation during epitaxy. It is expected that the model in question should apply to a broad class of DMS, as well as semiconductors and insulators, in which a constituent, dopant, or defect can exist in different charge states under various growth conditions.

An important example is $(\text{Ga},\text{Mn})\text{N}$, in which remarkable changes in ferromagnetic characteristics on co-doping with shallow impurities have recently been reported⁷⁵. In particular, a strong dependence of saturation magnetization M_s at 300 K on co-doping with Si donors and Mg acceptors⁷⁵ has been found for $(\text{Ga},\text{Mn})\text{N}$ with an average Mn concentration x of about 0.2%. In the case of $(\text{Zn},\text{Cr})\text{Te}$, a ferromagnetic response persists up 300 K for $x = 0.2$, according to both magnetization and magnetic circular dichroism measurements (Fig. 12). The ferromagnetism of $(\text{Zn},\text{Cr})\text{Te}$ is destroyed by N acceptor doping⁷⁷, an effect illustrated in Fig. 13 for $x = 0.01$.

Both double exchange and superexchange are inefficient at the low Mn and Cr concentrations for the midgap transition metal levels in question. At the same time, the model of nanocrystal self-organized growth⁷⁴ appears to explain why ferromagnetism appears when transition metal impurities are in the neutral charge state and vanishes when co-doping by shallow impurities cause the transition metal atoms to be electrically charged.

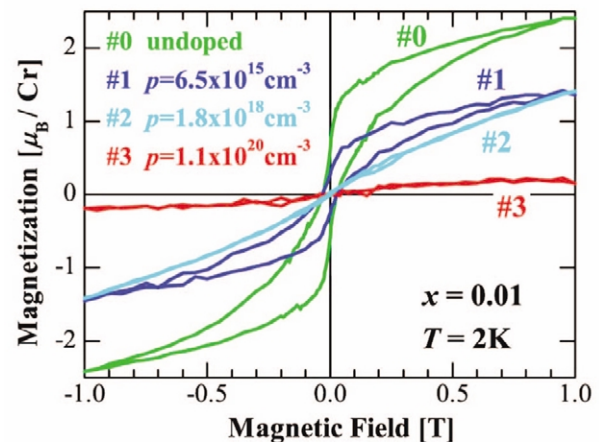


Fig. 13 Effect on magnetization of $\text{Zn}_{0.99}\text{Cr}_{0.01}\text{Te}$ doping by N acceptors. (Adapted and reprinted with permission from⁷⁷. © 2005 American Institute of Physics.)

Conclusions

In tetrahedrally coordinated semiconductors, strong hybridization between the open d shells of substitutional magnetic impurities and the p orbitals of neighboring anions results in an elevated T_C , even for small densities of magnetic ions, provided that the hole concentration is sufficiently high. In these carrier-controlled DMS, co-doping by donors and acceptors, light, electric fields, and electric currents can manipulate the ordering temperature and magnetization direction. It is remarkable that these outstanding functionalities of $(\text{Ga},\text{Mn})\text{As}$, $p\text{-(Cd},\text{Mn})\text{Te}$, and related quantum structures can be satisfactorily explained within the $p\text{-}d$ Zener model, if pertinent characteristics of the valence band, such as a strong spin-orbit interaction and anisotropy, are thoroughly taken into account.

Further progress, particularly the increase of T_C above room temperature, requires the development of DMS, especially nitrides and oxides, with higher magnetic ion and hole concentrations. We are

beginning to realize that positioning the Fermi level during growth and postgrowth processing constitutes an important means to affect self-compensation and solubility limits. In particular, an appropriate magnetic ion charge state, determined by the Fermi energy, can block spinodal decomposition and the associated aggregation of the magnetic ions. Alternatively, the controlled self-organized growth of magnetic nanocrystals can result in composite materials with enhanced magneto-optical and magnetotransport characteristics. High-density, three-dimensional memories and spatial light modulators for advanced photonic devices are examples of possible applications for these novel systems. 

Acknowledgments

The work of TD was supported in part by the European Commission NANOSPIN project (FP6-2002-IST-015728), the Humboldt Foundation, and carried out in collaboration with M. Sawicki and P. Kossacki in Warsaw, Poland and the groups of A. Bonanni in Linz, Austria, J. Cibert in Grenoble, France, B. Gallagher in Nottingham, UK, S. Kuroda in Tsukuba, Japan, and L. W. Molenkamp in Würzburg, Germany. The work of HO was supported in part by the IT Program RR2002 from MEXT and the 21st century COE program at Tohoku University, Japan.

REFERENCES

- Ohno, H., et al., *JSAP Int.* (2002) **5**, 4
- Wolf, S. A., et al., *Science* (2001) **294**, 1488
- Dietl, T., *Acta Phys. Pol., A* (2001) **100** (suppl.), 139; cond-mat/0201279
- Zutic, I., et al., *Rev. Mod. Phys.* (2004) **76**, 323
- Dietl, T., *Semicond. Sci. Technol.* (2002) **17**, 377
- Ohno, H., et al., *Phys. Rev. Lett.* (1992) **68**, 2664
- Ohno, H., et al., *Appl. Phys. Lett.* (1996) **69**, 363
- Dietl, T., et al., *Phys. Rev. B* (1997) **55**, R3347
- Haury, A., et al., *Phys. Rev. Lett.* (1997) **79**, 511
- Ferrand, D., et al., *Phys. Rev. B* (2001) **63**, 085201
- Ohno, H., et al., *Nature* (2000) **408**, 944
- Dietl, T., et al., *Science* (2000) **287**, 1019
- Pearson, S. J., et al., *J. Appl. Phys.* (2003) **93**, 1
- Prellier, W., et al., *J. Phys.: Condens. Matter* (2003) **15**, R158
- Dietl, T., In: *Proc. 27th Int. Conf. Phys. Semicond.*, Menéndez, J., and Van de Walle, C. G., (eds.), AIP, Melville, (2005), 56; cond-mat/0408561
- Liu, C., et al., *J. Mater. Sci.* (2005) **16**, 555
- Fukumura, T., et al., *Semicond. Sci. Technol.* (2005) **20**, S103
- Jungwirth, T., et al., *Rev. Mod. Phys.* (2006) **76**, 725
- Coey, J. M. D., *J. Appl. Phys.* (2005) **97**, 10D313
- Abraham, D. W., et al., *Appl. Phys. Lett.* (2005) **87**, 252502
- Dietl, T., In: *Handbook on Semiconductors*, Moss, T. S., (ed.), Elsevier, Amsterdam, The Netherlands, (1994), **3B**, 1251
- Kepa, H., et al., *Phys. Rev. Lett.* (2003) **91**, 087205
- Matsukura, F., et al., *Phys. Rev. B* (1998) **57**, R2037
- König, J., et al., *Phys. Rev. B* (2001) **64**, 184423
- Szczytko, J., et al., *Phys. Rev. B* (1999) **60**, 8304
- Fedorych, O. M., et al., *Phys. Rev. B* (2002) **66**, 045201
- Mizokawa, T., et al., *Phys. Rev. B* (2002) **65**, 085209
- Rader, O., et al., *Phys. Rev. B* (2004) **69**, 075202
- Hwang, J. I., et al., *Phys. Rev. B* (2005) **72**, 085216
- Dietl, T., et al., *Phys. Rev. B* (2001) **63**, 195205
- Abolfath, M., et al., *Phys. Rev. B* (2001) **63**, 054418
- Vurgaftman, I., and Meyer, J. R., *Phys. Rev. B* (2001) **64**, 245207
- Sankowski, P., and Kacman, P., *Phys. Rev. B* (2005) **71**, 201303(R)
- Timm, C., and MacDonald, A. H., *Phys. Rev. B* (2005) **71**, 155206
- Dietl, T., *J. Phys.: Condens. Matter* (2004) **16**, S5471
- Sankowski, P., et al., *Phys. Rev. B* (2006), submitted; cond-mat/0607206
- Jungwirth, T., et al., *Phys. Rev. B* (2005) **72**, 165204
- Boukari, H., et al., *Phys. Rev. Lett.* (2002) **88**, 207204
- Kechrakos, D., et al., *Phys. Rev. Lett.*, (2005) **94**, 127201
- Jaroszynski, J., et al., *Phys. Rev. Lett.* (2006), submitted; cond-mat/0509189
- Andrearczyk, T., et al., In: *Proc. 25th Int. Conf. Phys. Semicond.*, Miura, N., and Ando, T., (eds.), Springer, Berlin, Germany, (2001), 235
- Jaroszynski, J., et al., *Phys. Rev. Lett.* (2002) **89**, 266802
- Kohda, M., et al., *Appl. Phys. Lett.* (2006) **89**, 012103
- Koshihara, S., et al., *Phys. Rev. Lett.* (1997) **78**, 4617
- Chiba, D., et al., *Phys. Rev. Lett.* (2004) **93**, 216602
- Elsen, M., et al., *Phys. Rev. B* (2006) **73**, 035303
- Yamanouchi, M., et al., *Nature* (2004) **428**, 539
- Yamanouchi, M., et al., *Phys. Rev. Lett.* (2006) **96**, 096601
- Dietl, T., et al., *Phys. Rev. B* (2001) **64**, 241201
- Sawicki, M., et al., *Phys. Rev. B* (2004) **70**, 245325
- Matsukura, F., et al., III-V ferromagnetic semiconductors, In *Handbook of Magnetic Materials*, Buschow, K. H. J., (ed.), Elsevier, Amsterdam, The Netherlands, (2002) **14**, 1
- Wang, K., et al., In: *Proc. 27th Int. Conf. Phys. Semicond.*, Menéndez, J., and Van de Walle, C. G., (eds.), AIP, Melville, (2005) 333
- Ku, K. C., et al., *Appl. Phys. Lett.* (2003) **82**, 2302
- Chiba, D., et al., *Appl. Phys. Lett.* (2003) **82**, 3020
- Adell, M., et al., *Appl. Phys. Lett.* (2005) **86**, 112501
- Yu, K. M., et al., *Phys. Rev. B* (2002) **65**, 201303
- De Boeck, J., et al., *Appl. Phys. Lett.* (1996) **68**, 2744
- Mašek, J., and Máca, F., *Acta Phys. Pol., A* (2001) **100**, 319
- Blinowski, J., and Kacman, P., *Phys. Rev. B* (2003) **67**, 121204(R)
- Edmonds, K. W., et al., *Phys. Rev. Lett.* (2004) **92**, 037201
- Satoh Y., et al., *Physica E* (2001) **10**, 196
- Goennenwein, S. T. B., et al., *Phys. Rev. Lett.* (2004) **92**, 227202
- Wojtowicz, T., et al., *Appl. Phys. Lett.* (2003) **83**, 4220
- Yu, K. M. et al., *Appl. Phys. Lett.* (2004) **84**, 4325
- van Schilfgaarde, M., and Mryasov, O. N., *Phys. Rev. B* (2001) **63**, 233205
- Sato, K., et al., *Jpn. J. Appl. Phys.* (2005) **44**, L948
- Moreno, M., et al., *J. Appl. Phys.* (2002) **92**, 4672
- Yokoyama, M., et al., *J. Appl. Phys.* (2005) **97**, 10D317
- Martínez-Criado, G., et al., *Appl. Phys. Lett.* (2005) **86**, 131927
- Jamet, M., et al., *Nat. Mater.* (2006) **5**, 653
- Trohidou, K. N., et al., *Phys. Status Solidi A* (2002) **189**, 305
- Ye, S., et al., *Appl. Phys. Lett.* (2003) **83**, 3927
- Shinde, S. R., et al., *Phys. Rev. Lett.* (2004) **92**, 166601
- Dietl, T., *Nat. Mater.* (2006) **5**, 673
- Reed, M. J., et al., *Appl. Phys. Lett.* (2005) **86**, 102504
- Saito, H., et al., *Phys. Rev. Lett.* (2003) **90**, 207202
- Ozaki, N., et al., *Appl. Phys. Lett.* (2005) **87**, 192116